11-1-2021

A calorimetric, volumetric and combined SANS and SAXS study of hybrid siloxane phosphocholine bilayers

Mark B. Frampton
Brock University

Doruntina Yakoub
University of Windsor

John Katsaras
Oak Ridge National Laboratory

Paul M. Zelisko
Brock University

Drew Marquardt
University of Windsor

A Calorimetric, Volumetric and Combined SANS and SAXS Study of Hybrid Siloxane Phosphocholine Bilayers

Mark B. Frampton,[a,b,j,*] Doruntina Yakoub,[c] John Katsaras,[d,e,f,g,h] Paul M. Zelisko,[a,b] and Drew Marquardt [c,i,*]

[a] *Department of Chemistry and Centre for Biotechnology, Brock University, St. Catharines, ON, Canada*

[b] *Advanced Biomanufacturing Centre, Brock University, St. Catharines, ON, Canada*

[c] *Department of Chemistry and Biochemistry, University of Windsor, Windsor, ON, Canada*

[d] *Labs and Soft Matter Group, Neutron Scattering Division, Oak Ridge National Laboratory, Oak Ridge, TN, USA*

[e] *The Bredesen Center, University of Tennessee, Knoxville, TN, USA*

[f] *Shull Wollan Center, Oak Ridge National Laboratory, Oak Ridge, TN, USA*

[g] *Department of Physics, Brock University, St. Catharines, ON, Canada*

[h] *Department of Physics and Astronomy, University of Tennessee, Knoxville, TN, USA*

[i] *Department of Physics, University of Windsor, Windsor, ON, Canada*

[j] *Current address: School of Biosciences, Loyalist College, Belleville, ON, Canada*

* *Corresponding authors*

Abstract

Siloxanes are molecules used extensively in commercial, industrial, and biomedical applications. The inclusion of short siloxane chains into phospholipids results in interesting physical properties, including the ability to form low polydispersity unilamellar vesicles. Moreover, hybrid siloxane phosphocholines (SiPCs) have been examined as a potential platform for the delivery of therapeutic agents. Using small angle X-ray and neutron scattering, vibrating tube densitometry, and differential scanning calorimetry, we studied four hybrid SiPCs bilayers. Lipid volume measurements for the different SiPCs (i.e., 1124.3 Å^3, 1300.3 Å^3, 1394.3 Å^3, and 1306.6 Å^3) compared well with those previously determined for polyunsaturated PCs. Furthermore, the different SiPC's membrane thicknesses increased monotonically with temperature and, for the most part, a behavior also observed in unsaturated lipids, such as 1-palmitoyl-2-docosahexaenoyl-

sn-glycero-3-phosphocholine and 1-stearoyl-2-docosahexaenoyl-*sn*-glycero-3-phosphocholine, and the branched lipid 1,2-diphytanoyl-*sn*-glyerco-3-phosphocholine (DPhyPC).

Abbreviations

1,2-SiPC – 1,2-di(10-(1,1,3,3,3-pentamethyldisiloxanyl)decanoyl)-*sn*-glycero-2-phosphocholine; 1,3-SiPC – 1,3-di(10-(1,1,3,3,3-pentamethyldisiloxanyl)decanoyl)-*sn*-glycero-3-phosphocholine; DPhyPC - 1,2-diphytanoyl-*sn*-glyerco-3-phosphocholine; POPC - 1-palmitoyl-2-oleoyl-*sn*-glycero-3-phosphocholine; DOPC - 1,2-dioleoyl-*sn*-glycero-3-phosphocholine; DPPC – 1,2-dipalmitoyl-*sn*-glycero-3-phosphocholine; PDPC- 1-palmitoyl-2-docosahexaenoyl-*sn*-glycero-3-phosphocholine; SDPC - 1-stearoyl-2-docosahexaenoyl-*sn*-glycero-3-phosphocholine; SAXS – small angle X-ray scattering; SANS – small angle neutron scattering; PalValDSPC – 1-palmitoyl-2-(5-(1,1,3,3,3-pentamethyldisiloxanyl)pentanoyl)-*sn*-glycero-3-phosphocholine; PalCpcDSPC - 1-palmitoyl-2-(10-(1,1,3,3,3-pentamethyldisiloxanyl)decanoyl)-*sn*-glycero-3-phosphocholine; PalCpcTSPC - 1-palmitoyl-2-(10-(1,1,3,3,5,5,5-heptamethyltrisiloxanyl)decanoyl)-*sn*-glycero-3-phosphocholine; OleCpcDSPC - 1-oleoyl-2-(10-(1,1,3,3,3-pentamethyldisiloxanyl)decanoyl)-*sn*-glycero-3-phosphocholine; PCs – phosphocholines; SiPCs – siloxane phosphocholines.

Introduction

Siloxanes are compounds with a variety of industrial and cosmetic uses, and are sought after for their biocompatibility and other physicochemical properties that result from the unique nature of their dimethylsiloxy group.[1,2] Lipids containing a silicon atom were first prepared in 1987 by Thompson and co-workers,[3] but it would take another 30 years before the first siloxane-containing phosphocholines were synthesized and studied[4] – this is surprising considering the amount of research that has been dedicated to siloxane surfactants, [5-9] which share many characteristics with phospholipids, including the ability to self-assemble when introduced to water. Importantly, by combining the physicochemical features of organic and siloxane surfactants into a single molecule, new insights into the development of novel materials of industrial and commercial relevance may arise. Hybrid siloxane phosphocholines (SiPCs) with a siloxane chain attached to a phosphocholine lipid molecule may be a significant step toward this direction.[10,11]

Liposomes are frequently used as cellular mimics to study the biophysical interactions between lipids, proteins, and other substrates. [12] In the last few decades, self-assembled

phospholipid liposomes have become attractive vehicles for drug delivery, due to their biocompatibility, inherent low toxicity, and their ability to encapsulate both hydrophilic or hydrophobic therapeutics, including the recently developed mRNA vaccines.[12,13,14] Phospholipids dispersed in aqueous media self-assemble into spherical vesicles, typically with multi lamellar morphologies. However, the lamellarity of liposomes can be controlled, to various degrees, by incorporating charged lipids, or lipids with differing chain lengths.[15,16] The synthetic lipid, 1,2-diphytanoyl-*sn*-glyerco-3-phosphocholine (DPhyPC) forms unilamellar vesicles (ULVs) so long as the amount of DPhyPC is greater than 50 mol% of the total phospholipid compliment.[17] Non-natural phospholipids, such as those connecting their acyl chains to their glycerol backbones through amide linkages, can also self-assemble into cuboid morphologies whose acyl chains are known to interdigitate.[18,19] For example, PCs possessing trisiloxanes self-assemble into low polydispersity ULVs.[10] Hybrid SiPCs possessing a C_8-C_{14} alkyl fatty acid chain in their *sn*-1 position and a short disiloxane fatty acid in their *sn-2* position, also form ULVs, but an increase of their fatty acid chain lengths to C_{16} or C_{18} results in multilamellar vesicles (MLVs).[11] As chain length mismatch becomes larger, the propensity for fatty acid chain interdigitation between the inner and outer leaflet lipids also increases.

The thermotropic behaviour of siloxane PCs is unlike what is observed for saturated acyl chain PCs with similar chain lengths, and more closely resembles the thermotropic behaviour of unsaturated PCs. Differential scanning calorimetry (DSC) measurements of several SiPCs produced featureless thermograms between 5°C and 60°C, with the exception of a stearic acid-containing hybrid SiPC that showed a weak phase transition near 16.8°C.[11] The structure of the siloxane moiety disrupts acyl chain packing within the bilayer and the low barrier to linearization of the Si-O-Si linkage, which is only 1.26 kJ/mol (0.3 kcal/mol), has greater fluidity than pure alkyl chains.[20] Moreover, the pendant methyl groups on silicon are reminiscent of the phytanoic acid tails in DPhyPC, which is also found in the fluid phase over an extended range of temperatures.[21,22]

Siloxane PCs with two siloxane chains have a larger cross-sectional area per lipid and lipid volume than saturated PCs with similar chain lengths. The dimethylsilyl groups account for much of the increased area that arises from both steric and dynamic contributions. Bonding between silicon and other atoms also results in longer bonds and larger bond angles. For example, the average Si-O (1.63 Å) and Si-C bonds (1.87 Å) are longer than the average C-C bond (1.54 Å), and Si-O-Si bond angles can extend to 145°, compared to tetrahedral C-C-C bond angles of

109.5°.[1] These molecular characteristics impart a larger free volume to siloxane groups compared to pure alkyl chains. As a result, the cross-sectional areas, at 20°C, for the siloxane lipids 1,2-SiPC and 1,3-SiPC are 69±2 Å^2 and 72±4 Å^2,[10] respectively, compared to 62.7±2 Å^2 for POPC at 20°C.[43]The lipid volumes for double-tailed SiPCs (1574 Å^3 and 1577Å^3) are ~15-20% larger than POPC (1247 Å^3) and PDPC (1296.6 Å^3),[23] and ~10% larger than DPhyPC (1425 Å^3),[43] highlighting the steric contributions that result from the siloxane moiety. Hybrid SiPCs with short *sn-2* chains possess a smaller volume than their double-tailed counterparts, and range in volume from 923 Å^3 -1180 Å^3.[11]

Here, we present a combined SAXS and SANS study of four hybrid SiPCs, namely PalValDSPC (**1**), PalCpcDSPC (**2)**, PalCpcTSPC (**3)**, OleCpcDSPC (**4**) (**Figure 1**) in order to study and compare their morphologies and structural properties to their PC counterparts specifically, area per lipid, lipid volume, and membrane thickness.

Experimental

Synthesis of Siloxane Phosphocholines.

Siloxane phosphocholines **1-3** were prepared as described in reference 11, and their spectroscopic analyses were consistent with those in literature – detailed synthetic procedures and spectroscopic characterization for SiPC **4** are described in the Supporting Information. SiPCs were synthesized using a two-step approach. Firstly, lyso-PCs were prepared by melting palmitic acid or oleic acid with α-glycerophosphocholine in the presence of 10% w/w of N435, providing access to 16:0 or 18:1 lyso-PCs. Of note, is that phosphoryl migration is known to occur during the synthesis of lyso-PCs and can result in the cyclization of the phosphate group and subsequent elimination of the choline moiety, resulting in a cyclic phosphatidic acid, or the migration of the phosphocholine group from the *sn-3* to the *sn-2* position of the glycerol backbone.[24,25] Proton-decoupled ^{31}P-NMR spectra of lyso-PCs exhibited a single resonance, with a ^{31}P NMR chemical shift comparable to that observed in standard samples of lyso-PCs, indicating that all synthesized lyso-PCs retained their phosphocholine groups in the *sn-3* position. Additionally, there was little evidence found to suggest acyl migration between the *sn-1* and *sn-2* positions, which has been suggested to occur, albeit with low frequency. Lyso-PCs were then further elaborated on using a Steglich

esterification, resulting in the hybrid SiPCs **1**-**4**. Spectroscopic characterization of the SiPCs was in agreement with previous reports.[11,26]

Liposomes for SANS and SAXS Measurements.

ULVs composed of SiPCs were prepared by hydrating thin films of lipids formed on the walls of glass vials by transferring stock lipid solutions to glass vials and then removing the chloroform using a stream of argon gas and gentle heating (~25ºC). Residual solvent was removed by placing samples under vacuum for no less than 8 h. Dried lipid films were then hydrated with 100% D_2O –MLVs – for SANS measurements, followed by 7 freeze-thaw-vortex cycles. ULVs were produced by extruding MLVs using 50 nm diameter LipX single use polycarbonate filters (T & T Scientific, Knoxville, TN). Other than being rinsed with D_2O, filters were used as received. Prior to small angle scattering experimentation, final vesicle size distribution was determined by dynamic light scattering (DLS). SANS samples were then divided into two aliquots and diluted to the desired external contrast condition (i.e., 100 and 75% D_2O) using the appropriate amounts of D_2O and/or H_2O to achieve a final lipid concentration of 12 mg/ml. The 100% D_2O sample was used for SAXS measurements.

Small Angle Neutron and X-Ray scattering.

SiPC ULVs were loaded into 1 mm path-length quartz banjo cells (Hellma USA, Plainview, NY) and mounted in a temperature-controlled cell holder. SANS measurements were performed at the High Flux Isotope Reactor (HFIR) CG-3 Bio-SANS instrument located at Oak Ridge National Laboratory (ORNL). Data were collected at a sample-to-detector distance (SDD) of 7 meters using 6 Å wavelength neutrons (FWHM of 15%). Scattered neutrons were detected using a 1 m x 1 m two-dimensional (192 x 192 pixel) ^{3}He position-sensitive detector (ORDELA, Inc., Oak Ridge, TN) and a 1 m x 0.8 m wing detector (160 x 256 pixel). The merged data from the two detectors resulted in a total scattering vector (**q**) of 0.007 - 0.90 $Å^{-1}$. Two-dimensional data were reduced into a one-dimensional scattering intensity (I) vs scattering vector (**q**) plot using ORNL's MANTID software.[27] SAXS data were measured with a Rigaku BioSAXS-2000 home source system with a Pilatus 100K detector and a HF007 copper rotating anode (Rigaku Americas, The Woodlands, TX) using a fixed capillary flow-cell. SAXS data were collected in 24, 10-min

snapshots, and the averaged one-dimensional scattering curves were generated using the SAXSLab software.

Volume Measurements.

Samples for volumetric measurements were prepared by hydrating 25 mg of SiPC films with 1.5 g of degassed ultra-pure water – obtained from a High-Q purification system (Wilmette, IL) – followed by incubation at 50 °C for 30 min with periodic vortexing (~every 10 min.). The temperature dependent density of water (ρ_w) and of the SiPC lipid dispersions (ρ_s) were determined by a temperature-controlled Anton-Paar DMA5000 (Graz, Austria) vibrating tube densitometer, using previously established data collection methods.[11,23,28] The lipid volume (V_L) for a given temperature was calculated as:

$$V_L = \frac{MW_L}{N_A m_L}\left(\frac{m_L + m_W}{\rho_s} - \frac{m_W}{\rho_w}\right),$$

where MW_L is the molecular weight of the lipid, N_A is Avogadro's number, and m_L and m_w are the masses of the lipid and water, respectively. The impact of temperature on lipid volume was further quantified by determining the thermal volume expansivity (α^T_V) for each of the lipids at a constant surface pressure (Π) as follows:[29]

$$\alpha_V^T = (\delta V/\delta T)_{\Pi}\, V^{-1}.$$

Differential Scanning Calorimetry (DSC).

SiPC liposomes for DSC were prepared by diluting thin films of lipid to a final concentration of ~1.6 mg/mL in ultra-pure water. 1,2-dipalmitoyl-*sn*-glycero-3-phosphocholine (DPPC) was included as a reference sample and was prepared at a concentration of 0.8 mg/mL. The thermal phase transitions of DPPC are well characterized, with pre-transition and main transition temperatures of 34°C and 41°C, respectively. DSC thermograms over a temperature range of between 3°C and 60°C were acquired using a Nano DSC (TA Instruments, New Castle, DE) and scan rates of 1.0, 0.5, 0.2 and 0.1 °C/min.

Dynamic Light Scattering (DLS).

ULVs were diluted more than 150-fold in 12 mm x 75 mm culture tubes and their size distribution measured using DLS. Autocorrelation curves were modelled using the cumulant analysis performed by the instrument software (Brookhaven Instruments, Holtsville, NY).[30]

RESULTS and DISCUSSION.

Differential Scanning Calorimetry.

Hybrid SiPCs liposomes were DSC to determine their thermotropic behaviour (**Figure 2**); DPPC was used as a standard phospholipid. By way of comparison, POPC's *sn*-2 fatty acid chain possesses a single double bond and the lipid has a thermal phase transition at -2°C, while 1,2-dioleoyl-*sn*-glycero-3-phosphocholine (DOPC), with two unsaturated fatty acid chains, has a gel-to-liquid phase transition at -17°C.[31] Despite SiPCs **1-3** possessing a palmitic fatty acid chain in their *sn*-1 positions, their thermograms did not exhibit a gel-to-liquid phase transition between 5°C and 60°C, [11] in agreement with what has previously been reported, including for vesicles with siloxane surfactants.[32] Knowing this, it was unsurprising that SiPC **4** with an oleic acid in its *sn-1* position did not show a phase transition over the temperature range studied. Siloxane fatty acids resemble the branched phytanoic acids found in DPhyPC, which do not have a demonstrable gel-to-liquid phase transition between -120°C and 120°C.[21] The absence of a thermal phase transition in SiPCs **1-4** is reflective of the degree of disorder in the membrane that is imparted by the siloxane subunits, and the resultant lower degree of packing taking place among their fatty acid tails.

Volume Measurements.

Lipid volume (V_L) is an important structural parameter used to evaluate the different structural parameters of lipid bilayers.[43,48] We used the vibrating tube densitometer protocol developed by Pan *et al.*[28] to determine the lipid volume (V_L) for each of the four hybrid SiPCs; for comparison we included POPC, a naturally occurring phospholipid. Lipid volumes, and volume expansivities are presented in **Table 1** and **Figure 2**.

For each SiPC examined, V_L increased with increasing temperature and a plot of V_L vs temperature did not show any discontinuities, suggesting that over the temperature range studied there was no gel-to-liquid phase transition; this observation was also supported by DSC data (**Figure *2***). At 30°C, SiPC **1** has a V_L of 1124.3 Å^3 and is the only lipid that has a volume smaller than POPC (V_L 1256.0 Å^3).[45] The remaining SiPCs at 30°C have volumes as follows: SiPC **2=**1300.3 Å^3, SiPC **3=** 1394.3 Å^3, and SiPC **4=** 1306.6 Å^3. All SiPCs have volumes larger than POPC and the saturated PCs studied (**Table *2***). Increasing the length of the *sn-2* fatty acid from C_5 to C_{10} results in a significant increase in V_L, as expected. Increasing the siloxane group from a disiloxane to a trisiloxane, as in the case of SiPC **2** and **3**, increases the lipid volume by ~94 Å^3. Even though SiPC **4** has an oleic acid in the *sn-1* position, it has a V_L comparable to SiPC **2**.

From the V_L data, it is clear that the incorporation of short siloxane units into fatty acid tails increase SiPC volumes such that, they are comparable to polyunsaturated PCs like, for example, PDPC (V_L =1306.4 Å^3) and SDPC (V_L = 1366.4 Å^3) (**Table 2**).[23] Hybrid SiPCs are considerably smaller than their double-tailed trisiloxane-containing counterparts, which have V_L of 1574 Å^3 and 1577 Å at 20 ^{o}C^3.[10] The increased molecular volumes of hybrid SiPCs are, in part, related to the increased flexibility of the siloxane linkage and the added volume of the dimethylsiloxy groups. The hybrid SiPC volume expansivities (α_V^T) for SiPC 1-3 are quite comparable with those reported for conventional PC lipids, POPC for example, reported in Kučerka *et al.*[43] (2011). This observation is further consistent with an increased flexibility of the siloxane linkage and the added volume of the dimethylsiloxy groups. The thermal volume expansivity for SiPC **4** is nearly double that observed for SiPCs 1-**3** owing to the coupled interaction of the oleic acid moiety in the *sn-1* position and the siloxane acid in the *sn-2* position.

SANS and SAXS Analysis.

SANS and SAXS data were jointly analyzed using the EZ-SDP symmetric bilayer model in Vesicle Viewer[33], an online data analysis software (**Figure 3**). The EZ-SDP model is a five-slab model that breaks the bilayer down into two headgroup slabs, two methylene slabs and a terminal methyl slab. Since the lipid structure is parsed into these five-slabs the model applicable for a variety of different lipid structures, including our hybrid SiPCs. As with any model, there are potential deficiencies, in the case of our implementation one must be cognisant that the EZ-SDP model may struggle to recapitulate the chain length mis-match of our hybrid SiPCs; SiPC **1** in

particular. How the hybrid SiPCs are projected into the EZ-SDP model is illustrated in SI Figure 1 (refer to ref 33 for a thorough explanation of the EZ-SDP model). The area per lipid (A_L), headgroup-headgroup distance (D_{HH}), bilayer thickness (D_B), and hydrocarbon thickness ($2D_C$) were then determined (**Table 2**). With the exception of A_L – which is a variable fitting parameter – all other parameters were geometrically derived using A_L and the experimentally obtained lipid volumes.

The scattering data show SiPCs forming bilayers that have similar properties to fluid phase PC bilayers with similar fatty acid chains (**Table *2***). Although not common, we used the D_B ($2V_L/A_L$) to compare relative degrees of chain order using the SAXS data. In doing so, we found good agreement between D_B and the average C-D order parameter (S_{CD}) determined by ^{2}H-NMR, shown in the top panel to **Figure 4**. SiPCs also have a similar degree of chain order when compared to mixed chain polyunsaturated fatty acid (PUFA)-containing PCs, but they are significantly more ordered than the branched-chain DiPhyPC, with the exception of SiPC **1** (**Figure 4**). Indeed, there is no fundamental law demanding that our hybrid SiPCs follow the trends of conventional phospholipids; however, the impact of chain dynamics on the geometry of the bilayer should be invariant to what chemical groups are inducing the disorder within the chains. The lipid shape parameter is an example of how lipid parameters are deconstructed into geometric parameters regardless of the lipid chain chemistry.[34] We note that the upper panel of **Figure 4** was constructed from S_{CD} derived from NMR and independently derived D_B from SAXS/SANS data. Furthermore, we observed a monotonic increase in A_L as a function of temperature for SiPCs, not unlike what was observed for other PC lipids. In contrast, the different SiPC thicknesses (D_B, D_{HH}, and $2D_C$) did not change with temperature as was observed in their PC counterparts (**Figure 5**). This would suggest that the increased A_L and relative acyl chain disorder are induced by the Si-containing acyl chain, as the *sn-1* acyl chain is expected to remain relatively unaffected by temperature. Siloxanes also exhibit a higher degree of vibrational and rotational freedom compared to the fatty acid chains found in natural phospholipids, owing to longer Si-O and Si-C bond lengths and larger bond angles, which allow for local regions of increased volume around the silicon atoms, resulting in greater siloxane moiety movement.[35] Moreover, the weak repulsive interactions between the silicon methyl groups leads to less well-packed acyl chains, thus the larger V_L values for SiPCs compared to PCs.[36]

In particular, SiPC **1,** previously analyzed using the Global Analysis Program (GAP) model developed by Pabst *et al.*,[37,38] exhibited unusually small bilayer thicknesses, the result of potential

partial chain interdigitation across the bilayer or chain bending into its respective leaflet. Using the SDP model, we found that SiPC **1** has a D_{HH} = 30.0 Å, a value comparable to the 28.26 Å[11]determined using the GAP model, while the other three SiPCs had D_{HH} values of 36.0 Å (SiPC **2**), 38.0 Å (SiPC **3**), and 36.8 Å (SiPC **4**). By comparison, DPPC and POPC had D_{HH} values of 38.4 Å and 36.5 Å, respectively. As mentioned, the "thin" SiPC **1** bilayer was the result of chain interdigitation or chain bending, features commonly observed in bilayers with mixed chain length lipids.[39,40,41] Given the large chain length mismatch of SiPC **1**, and the recent work on the interdigitation of chain-asymmetric PCs, it is most likely that there is a combination of interdigitation and chain bending backwards.[41] The work of Frewein *et al*. demonstrates through both SANS/SAXS measurements and specifically MD simulations, that there is a high fraction of chains bending back towards their own headgroup. Moreover, the bilayer thickness of SiPC **1** results in an unusually large A_L that can be rationalized by the chain length mismatch which induces disorder in the longer of the chains. In other words, the short chain induces disorder in the longer. The terminal methyl behaviour of our hybrid SiPC is largely speculation based on only the SAS data since we do not have MD simulations to support our interpretation (force fields currently do not exist for SiPC lipids). Our observation of a thinning membrane is driven by chain mismatch is consistent with the notion that chain length mismatch impacts hydrocarbon chain ordering by inducing disorder in the longer of the two hydrocarbons, 16:0 in our case.

A_L values for SiPCs **2-4** were larger than those of POPC and DPPC, but are comparable to values for PUFA-PCs, such as PDPC and SDPC (**Table 2**). Moreover, A_L values for SiPCs **2-4** are similar and significantly smaller than the A_L value for DPhyPC (**Table *2***). These data can be attributed to the siloxanes decorated fatty acids, and as previously suggested, behaved similarly to monounsaturated PCs – our analysis suggests that a better comparison would be PUFA-PCs.

Conclusions.

We synthesized four hybrid SiPCs with different siloxane fatty acids in their *sn-2* position and characterized their self-assembled bilayers. DSC measurements did not show the presence of a thermal phase transition in any of the SiPCs studied, implying that the attached siloxane groups disorder the bilayer to an extent that the bilayers remain in the same phase for the temperature range studied. This observation was borne out by volumetric measurements, where a plot of V_L vs

temperature did not show any discontinuities. In addition to calorimetric and volumetric measurements, SiPCs bilayers were interrogated using a combination of SANS and SAXS. Joint refinement analysis of the scattering data showed that the SiPCs studied are, in many respects, similar in structure to phosphocholines containing polyunsaturated chains. The increased fluidity imparted by the siloxane groups allows SiPC bilayers to remain in the fluid phase under physiologically relevant conditions.

Conflicts of Interest.

The authors have no conflicts of interest to declare.

Acknowledgements.

SANS studies on Bio-SANS were supported by the OBER funded Center for Structural Molecular Biology (CSMB) under Contract FWP ERKP291, using the High Flux Isotope Reactor, a DOE Office of Science User Facility operated by the Oak Ridge National Laboratory (Oak Ridge, Tennessee, USA). JK is supported through the Scientific User Facilities Division of the Department of Energy (DOE) Office of Science, sponsored by the Basic Energy Science (BES) Program under Contract DEAC05-00OR22725. DM acknowledges support from the Natural Sciences and Engineering Research Council (NSERC). PMZ acknowledges support from the Natural Sciences and Engineering Research Council (NSERC) and the Advanced Biomanufacturing Centre (ABC) at Brock University.

Figures and Tables.

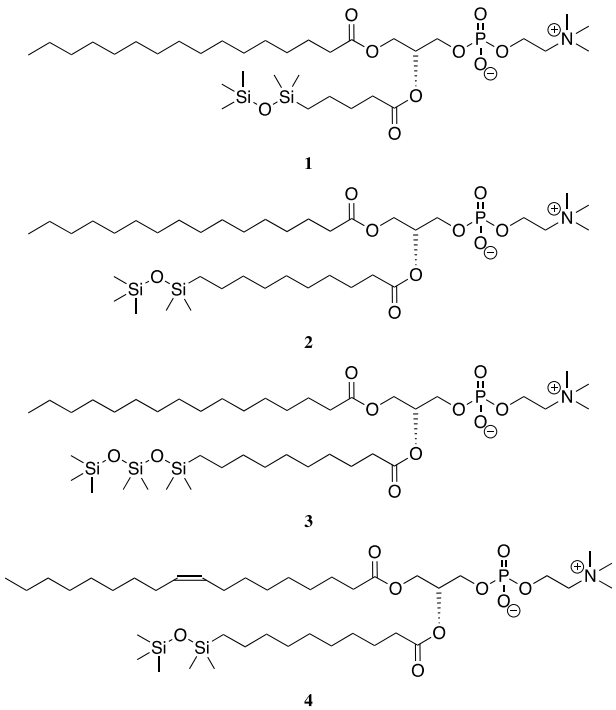

Figure 1 Structures of the siloxane phosphocholines **1-4** studied.

Table 1 Lipid volumes (V_L) and volume expansivities (α_T^V) of the different SiPCs. Estimated uncertainties are below ±1 %.

	PalValDSPC (**1**) [11]		PalCpcDSPC (**2**)		PalCpcTSPC (**3**)		OleCpcDSPC (**4**)	
TEMP (°C)	V_L (Å^3)	α_V^T (10^{-4}/°C)	V_L (Å^3)	α_V^T (10^{-4}/°C)	V_L (Å^3)	α_V^T (10^{-4}/°C)	V_L (Å^3)	α_V^T (10^{-4}/°C)
10	1103.0	8.4	1278.8	7.6	1369.4	8.0	1278.5	14.7
15	1108.6	8.3	1284.1	7.6	1375.8	8.0	1284.8	14.6
20	1114.9	8.3	1290.4	7.6	1383.2	7.9	1293.6	14.5
25	1119.9	8.2	1295.8	7.5	1389.1	7.9	1306.8	14.3
30	1124.3	8.2	1300.3	7.5	1394.3	7.9	1306.6	14.4
35	1128.5	8.2	1305.1	7.5	1399.3	7.8	1312.0	14.3
40	1133.1	8.1	1309.8	7.4	1404.8	7.8	1321.9	14.2
45	1137.2	8.1	1314.5	7.4	1409.7	7.8	1331.5	14.1
50	1141.8	8.1	1319.4	7.4	1415.3	7.7	1345.9	13.9
55	1146.0	8.0	1323.4	7.4	1420.3	7.7	-	-
60	1149.7	8.0	1327.8	7.3	1424.8	7.7	-	-

Table 2 Average molecular volumes (V_L), molecular areas (A_L) and membrane thicknesses (D_{HH}) of the different fluid phase phosphocholines (PC) studied. Unless indicated, data correspond to samples at 30°C.

PC	**Temp.**	**V_L (Å^3)**	**A_L (Å^2)**	**D_B (Å)**	**D_{HH} (Å)**	**$2D_C$ (Å)**	**Model**	**Reference**
1		1124.3	71.0	31.4	30.0	22.3	EZ-SDP	This work
		1124.3			28.26		GAP	Ref. 11 (Frampton *et al*. 2018)
2		1300.3	66.9	38.6	36.0	29.0	EZ-SDP	This work
3		1394.3	68.8	40.2	38.0	30.87	EZ-SDP	This work
4		1306.6	69.6	37.3	36.8	28.1	EZ-SDP	This work
1,2-SiPC	20°C	1574	69		36.3		GAP	Ref. 10 (Frampton *et al*. 2017)
1,3-SiPC	20°C	1577	72		35.3		GAP	Ref. 10 (Frampton *et al*. 2017)
POPC		1256	64.4		36.5		Full SDP	Ref. 43 (Kučerka *et al*. 2011)
DOPC		1303	72.4	44.8	36.7	26.8	SDP	Ref. 42 (Pan *et al*. 2008)
DPPC	50°C	1228.5	63.1		38.4		Full SDP	Ref. 43 (Kučerka *et al*. 2011)
		1228.5	65.7	38.5	35.2	27.5	EZ-SDP	Ref. 44 (Marquardt *et al*.)
PDPC		1306.4	71.1		33.2		Full SDP	Ref. 23 (Marquardt *et al*. 2020)
SDPC		1366.4	70.4		35.2		Full SDP	Ref. 23 (Marquardt *et al*. 2020)
DPhyPC		1425.8	80.5		36.4		Full SDP	Ref. 45 (Tristram-Nagle *et al*. 2010)
		1426.7	80.5		36.4		Full SDP	Ref. 43 (Kučerka *et al*. 2011)

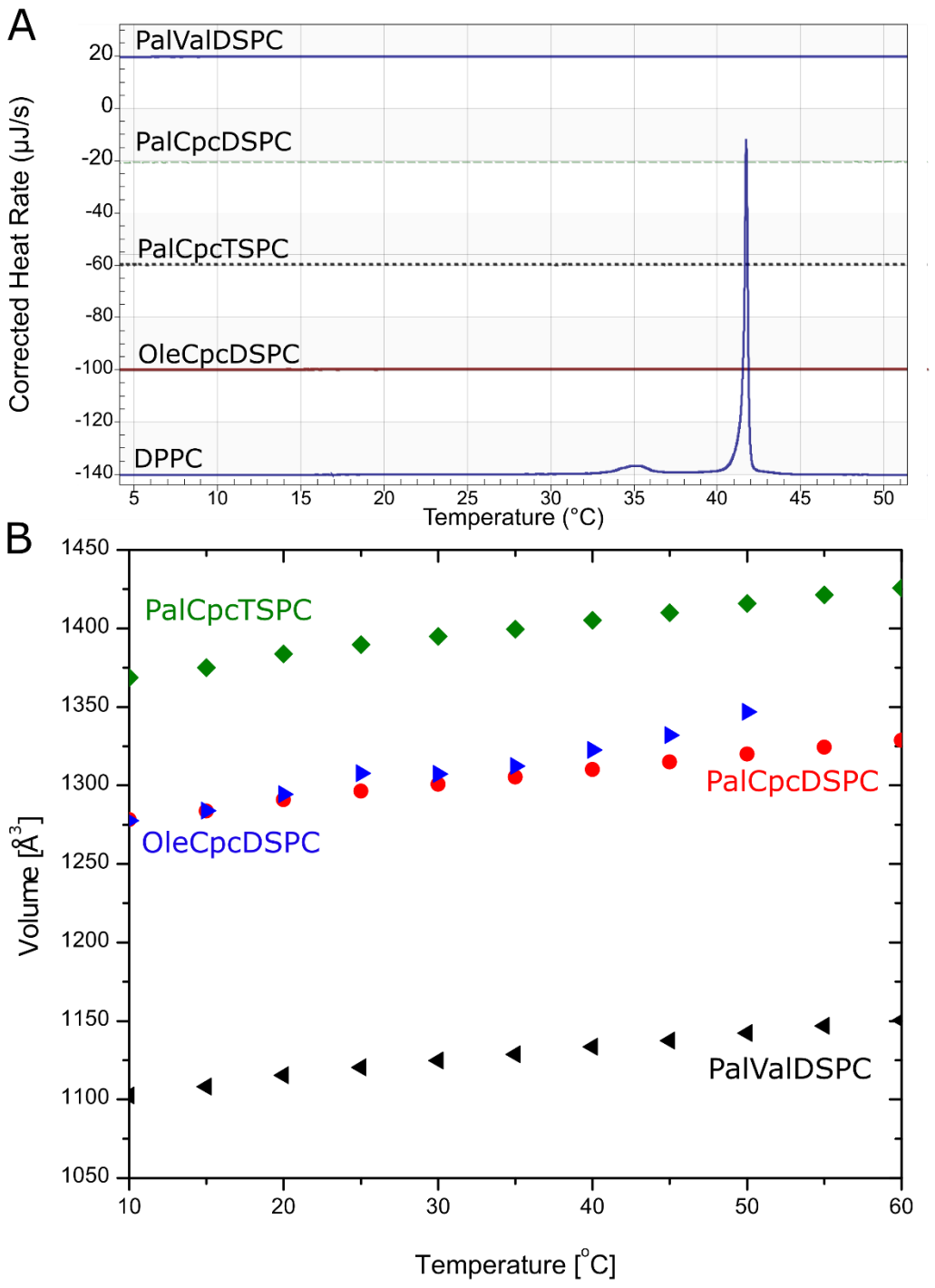

Figure 2 DSC thermograms (Panel A) and lipid volumes as a function of temperature (Panel B) of SiPC lipids, including DPPC (A). Estimated uncertainties are below the data point size (>1 %)

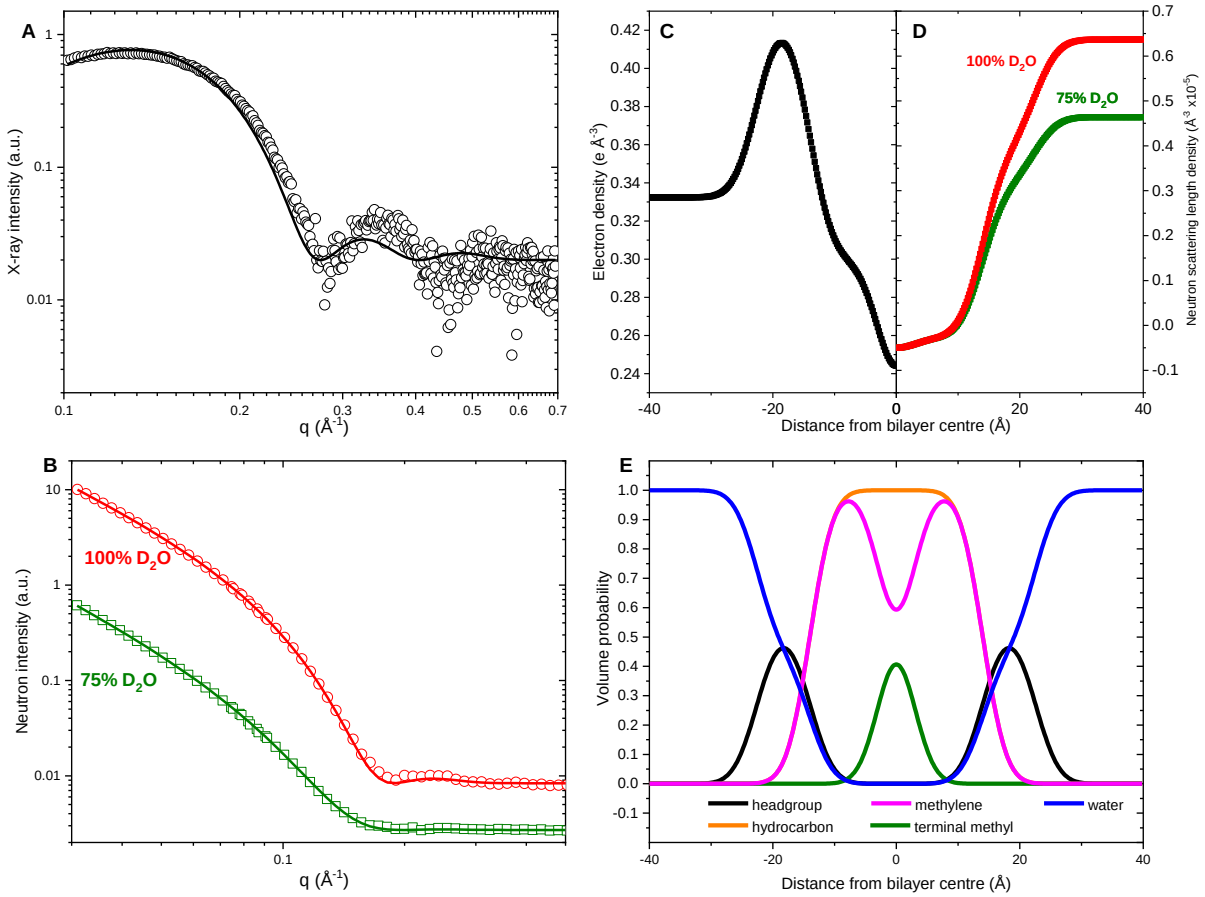

Figure 3 Fits (solid lines) to the experimental SAXS (Panel A) and SANS (Panel B) scattering data (points) for SiPC **4** (OleCpcDSPC) at 20°C using EZ-SDP. Note: SANS data was collected up to **q**=0.9 Å^{-1} and **q**=0.4-0.9 Å^{-1} is incoherent background. Panels C and D show the bilayer electron densities and neutron scattering length densities, respectively. Panel E illustrates the volume probability distributions of the key lipid structural features. Note that the total probability is equal to 1 at each point along the bilayer normal.

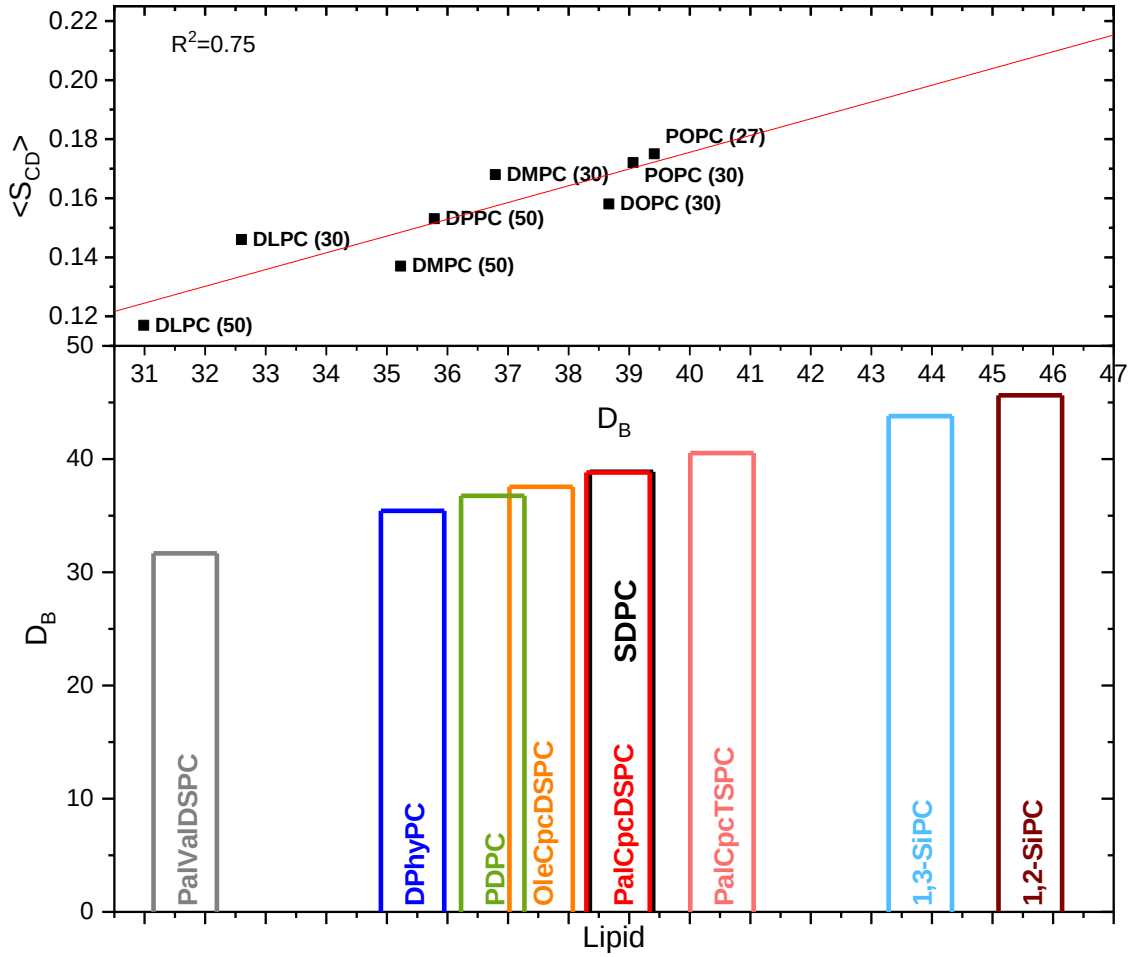

Figure 4 Top: The linear relationship between D_B and ^{2}H-NMR S_{CD} for common lipids are displayed. ^{2}H-NMR S_{CD} values are from Leftin and Brown[46] (POPC (27), DMPC and DLPC) and S_{CD} values for POPC (30) and DOPC are from Marquardt *et al.*[47]. D_B ($2V_L/A_L$) values were tabulated in Kučerka *et al.* [43], except for DOPC, which is from Kučerka *et al.* [48]. Bottom: D_B values for the different SiPCs studied and from those of representative lipids, i.e., PDPC,[23] SDPC[23] and DPhyPC[43]. Bottom panel, the lipids are arranged in increasing D_B values.

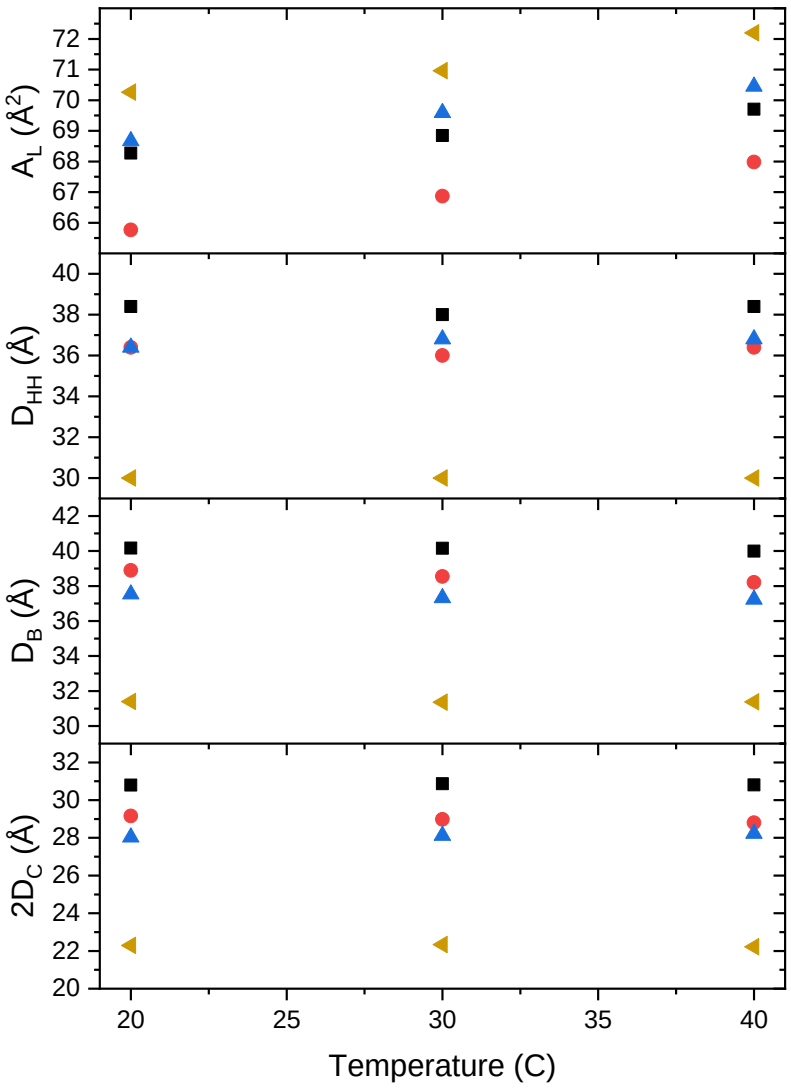

Figure 5 Different bilayer thicknesses of SiPCs **1-4** (**1** – gold triangles, **2** – red circles, **3** - black squares, **4** – blue triangles) bilayers.

References

[1] M.A. Brook. *Silicon in Organic, Organometallic and Polymer Chemistry*. Wiley. **2000**.

[2] Hill R.M. *Siloxane surfactants*. In: Robb I.D. (eds) *Specialist Surfactants*. Springer, **1997**.

[3] R.K. Kallury, U.J. Krull, and M. Thompson. *J. Org. Chem*., **1987**, *52*, 5478-5480.

[4] M.B. Frampton and P.M. Zelisko. *Eur. J. Lipid Sci. Technol*., **2017**, *119*, 1600248.

[5] I.D. Robb. *Specialist Surfactants*. Blackie Academic and Professional. **1997**.

[6] P.M. Zelisko, K.K. Flora, J.D. Brennan, and M.A. Brook. *Biomacromolecules*, **2008**, *9*, 2153-2161.

[7] M.A. Brook, P.M. Zelisko, M.J. Walsh, J.M. Crowley. *Silicon Chemistry*, **2002**, *1*, 99-106.

[8] H. Chen and J. Tan. *Langmuir*, **2020**, *36*, 14582-14588.

[9] Y. Huang, M. Guo, J. Tan, and S. Feng. *Langmuir*, **2020**, *36*, 2023-2029.

[10] M.B. Frampton, D. Marquardt, I. Letovsky-Papst, G. Pabst, and P.M. Zelisko. *Langmuir*, **2017**, *33*, 4948–4953.

[11] M.B. Frampton, M.H.L. Nguyen, M. DiPasquale, R. Dick, D. Marquardt, and P.M. Zelisko. *Chem. Phys. Lipids*, **2018**, *216*, 1-8.

[12] N. Maurer, D.B, Fenske, P.R. Cullis. *Expert Opin. Boil. Ther*., **2001**, *1*, 1–25.

[13] R. Cross. *Without these lipid shells, there would be no mRNA vaccines for COVID-19*, in Chemical and Engineering News, https://cen.acs.org/pharmaceuticals/drug-delivery/Without-lipid-shells-mRNA-vaccines/99/i8. **2021**.

[14] M. McCoy, *Lipids, the unsung COVID-19 vaccine component, get investment*, in Chemical and Engineering News, https://cen.acs.org/business/outsourcing/Lipids-unsung-COVID-19-vaccine/99/web/2021/02. **2021**.

[15] M.P. Nieh, T.A. Harroun, V.A. Raghunathan, C.J. Glinka, and J. Katsaras. *Phys. Rev. Lett*., **2003**, *19*, 158105.

[16] M.P. Nieh, J. Katsaras, and X. Qi. *Biochim. Biophys. Acta*, **2008**, *1778*, 1467–1471.

[17] M. Andersson, J. Jackman, D. Wilson, P. Jarvoll, V. Andersson, G. Okeyo, and R. Duran. *Coll. Surf. B: Biointerfaces*, **2011**, *82*, 550-561.

[18] F. Neuhaus, D. Mueller, R. Tanasescu, S. Balog, T. Ishikawa, G. Brezesinski, and A. Zumbuehl. *Angew. Chem. Int. Ed*., **2017**, *56*, 6515-6518.

[19] R. Tanasescu, M.A. Lanz, D. Mueller, S. Tassler, T. Ishikawa, R. Reiter, G. Brezesinski, and A. Zumbuehl. *Langmuir*, **2016**, *32*, 19, 4896–4903.

[20] M.A. Brook. *Silicon in Organic, Organometallic and Polymer Chemistry*. Wiley. **2000**.

[21] H. Lindsey, N.O. Petersen, and S.I. Chan. *Biochim. Biophys. Acta*, **1979**, *555*, 147–167.

[22] B.R. Lentz. *Chem. Phys. Lipids*, **1993**, *64*, 99−116.

[23] D. Marquardt, F.A. Heberle, J. Pan, X. Cheng, G. Pabst, T.A. Harroun, N. Kučerka, and J. Katsaras. *Chem. Phys. Lipids*, **2020**, *229*, 104892.

[24] P. D'Arrigo and S. Servi. *Molecules*, **2010**, *15*, 1354-1377.

[25] A. Plückthunt and E.A. Dennis. *Biochemistry*, **1982**, *21*, 1743-1750.

[26] P.A. Tongkoua Nkamou. *Siloxane Containing Phospholipids as Potential Drug Delivery Systems*. Brock University, **2019**.

[27] O. Arnold, J. Bilheux, J. Borreguero, A. Buts, S. Campbell, L. Chapon, M. Doucet, N. Draper, R. Ferraz Leal, M. Gigg, V. Lynch, A. Markvardsen, D. Mikkelson, R. Mikkelson, R. Miller, K. Palmen, P. Parker, G. Passos, T. Perring, P. Peterson, S. Ren, M. Reuter, A. Savici, J. Taylor, R. Taylor, R. Tolchenov, W. Zhou, and J. Zikovsky. *Nucl. Instr. Meth. Phys. Res. A*, **2014**, *764*, 156-166.

[28] J. Pan, F.A. Heberle, S. Tristam-Nagle, M. Szymanski, M. Koepfinger, J. Katsaras, and N. Kučerka. *Biochim. Biophys. Acta*, **2012**, *1818*, 2135-2148.

[29] H. Heerklotz and A. Tsamaloukas, *Biophys. J*., **2006**, *91*, 600-607.

[30] H. L. Scott, A. Skinkle, E. G. Kelley, M. N. Waxham, I. Levental and F. A. Heberle, *Biophys. J*., **2019**, *117*, 1381-1386.

[31] D. Marsh. *The Handbook of Lipid Bilayers, 2nd Edition*. CRC Press. **2013**.

[32] L.J. Petroff and S.A. Snow. *Silicone Surfactants*, in *Silicone Surface Science: Advances in Silicon Science 4*, M.J. Owen, P.R. Dvornic (Eds.), Springer Science+Business Media, **2012**.

[33] A. Lewis-Laurent, M. Doktorova, F.A. Heberle, and D. Marquardt. *Biophys. J*., **2021**, doi.org/10.1016/j.bpj.2021.09.018

[34] D. Marquardt, B. Geier, and G. Pabst. *Membranes*, **2015**, *5*, 180-196.

[35] C.E. Martin, G. Fardella, R. Perez, and J.W. Krumpfer, *Poly(siloxane)s, Poly(silazane)s, and Poly(carbosiloxane)s*, in *Functionalized Polymers: Synthesis, Characterization and Application*, Ed. N.P. Singh Chauhan, CRC Press. **2021**.

[36] J.E. Mark. *Acc. Chem. Res*., **2004**, *12*, 946-953.

[37] G. Pabst, M. Rappolt, H. Amenitsch, and P. Laggner. *Phys. Rev. E: Stat. Phys. Plasmas Fluids Relat. Interdiscip. Top. 62 (3 Pt B)*, **2000**, 4000–4009.

[38] G. Pabst, R. Koschuch, B. Pozo-Navas, M. Rappolt, K. Lohner, and P. Laggner. *J. Appl. Crystallogr*., **2003**, *36*, 1378–1388.

[39] C. Huang. *Klin Wochenshrift*, **1990**, *68*, 149–165.

[40] M.M. Batenjany, Z. Wang, C. Huang, and I.W. Levin. *Biochim. Biophys. Acta*, **1994**, *1192*, 205–214.

[41] M.P.K. Frewein, M. Doktorova, F.A. Heberle, H.L. Scott, E.F. Semeraro, L. Porcar, and G. Pabst. *Symmetry*, **2021**, *13*, 1441. https://doi.org/10.3390/sym13081441

[42] J. Pan, S. Tristam-Nagle, Norbert Kučerka, and J.F. Nagle. *Biophys. J*., **2008**, *94*, 117-124.

[43] N. Kučerka, M. Nieh, and J. Katasaras. *Biochim. Biophys. Acta Biomembr.*, **2011**, *1808*, 2761-2771.

[44] D. Marquardt, F.A. Heberle, T. Miti, B Eicher, E. London, J. Katsaras, and G. Pabst. *Langmuir*, **2017**, *33*, 15, 3731–3741.

[45] S. Tristram-Nagle, D.J. Kim, N. Akhunzada, N. Kučerka, J.C. Mathai, J. Katsaras, M. Zeidel, and J.F. Nagle. *Chem. Phys. Lipids*, **2010**, *163*, 630–637.

[46] A. Leftin and M.F Brown. *Biochim. Biophys. Acta Biomembr.*, **2011**, *1808*, 818-839.

[47] D. Marquardt, J.A. Williams, N. Kučerka, J. Atkinson, S.R. Wassall, J. Katsaras and T.A. Harroun. *J. Am. Chem. Soc*., **2013**, *135*, 7523−7533.

[48] N. Kučerka, J.F. Nagle, J.N. Sachs, S.E. Feller, J. Pencer, A. Jackson and J. Katasaras. *Biophys. J*., **2008**, *95*, 2356-2367.